

Fabrication of $\text{Cu}_2\text{ZnSnS}_4$ (CZTS) thin films by ultrasonic spray pyrolysis at a low substrate temperature and effect of tin concentration on the characteristics of the CZTS thin films

M. Sultana, A. Siddika, S. S. Mahmood, A. Sharmin, S. Tabassum, M. Rahaman and M. S. Bashar*

Bangladesh Council of Scientific and Industrial Research (BCSIR), Dhaka, Bangladesh

Abstract

$\text{Cu}_2\text{ZnSnS}_4$ (CZTS) thin films are fabricated on glass substrates using the spray pyrolysis method with different concentrations of Sn content were studied in this research work. All the CZTS thin films are fabricated at substrate temperature 200°C to minimize the formation of secondary phases. Here, we show how the variation in Sn content concentration influences the optical and structural properties of the CZTS thin films. The XRD patterns reveal that the concentration of Sn content has to be optimized to minimize the formation of secondary phases for a fixed substrate temperature. In turn, the band gap of the CZTS films is highly influenced by the formation of secondary phases. We have found that the films prepared from the precursor solution with 1.8 mM concentration of Sn content have the best crystal structure and an optical band gap of 1.55 eV. The CZTS thin films also have good carrier concentrations ranging from 4.2×10^{19} to $22.9 \times 10^{20} \text{ cm}^{-3}$.

Keywords: CZTS; Thin films; Spray Pyrolysis; Secondary phase; Carrier concentration; Low temperature

Received: 04 October 2021

Revised: 03 February 2022

Accepted: 08 February 2022

DOI: <https://doi.org/10.3329/bjisir.v57i1.58894>

Introduction

The highest efficiency of CIGS-based solar cells was 23.4% (Green *et al.*, 2019). Nevertheless, these cells utilize expensive and scarce elements like indium, limiting the mass production of solar cells based on these materials. These problems have stimulated the research for an alternative absorber layer based on earth-abundant materials. Scientists started to explore new materials like $\text{Cu}_2\text{ZnSnSe}_4$, $\text{Cu}_2\text{ZnSnS}_4$, and other quaternary of these chalcopyrite-like semiconductors. Indium and gallium used in CIGS thin-film solar cells were replaced with relatively cheap and abundant zinc and tin. Toxic selenium may be replaced with sulfur in $\text{Cu}_2\text{ZnSnS}_4$ (CZTS) thin-film solar cells. Furthermore, CZTS is a potential material for solar cell applications due to its good electrical and optical properties (Mitzi *et al.*, 2011), i.e., p-type conductivity, bandgap around 1.5 eV, and optical absorption coefficient around 10^{-4} cm^{-1} .

The spray pyrolysis method is one of the chemical methods to obtain the CZTS thin film layer. It is a low-cost method with the capability of significant area deposition. The composition, morphology, optical and electrical properties of the CZTS thin films can be tailored by changing deposition parameters such as the precursor source (Tanaka *et al.*, 2014), precursor concentration (Vigil-galán *et al.*, 2013; Vigil-galán *et al.*, 2015), substrate temperature (Babichuk *et al.*, 2018; Bhosale *et al.*, 2014), deposition time (Mahjoubi *et al.*, 2017), etc.

The Effect of tin concentration on films properties has been investigated in this research work and structural, morphological, and optical properties characterized the obtained CZTS thin films.

*Corresponding author e-mail: bashar@agni.com

Experimental

CZTS thin film deposition was performed by a pneumatic spray pyrolysis method in an air atmosphere with an ultrasonic spray nozzle. A precursor solution consisting of $\text{CuCl}_2 \cdot 2\text{H}_2\text{O}$, ZnCl_2 , $\text{SnCl}_4 \cdot 5\text{H}_2\text{O}$, and thiourea (with an intentional concentration in excess) was dissolved in distilled water. This solution was sprayed onto soda-lime glass substrates heated at 200°C . The nozzle to substrates distance was around 25 cm, and a total 1100 ml solution was sprayed continuously at a flow rate of 0.01 ml/sec. Air was used as the carrier gas during the spray deposition. To investigate the influence of the tin concentration on the properties of CZTS thin films, it was changed from 0.5 to 2.4 mM. The samples were denoted as S1 for tin concentration 0.5 mM, S2 for tin concentration 1.6 mM, S3 for tin concentration 1.8 mM, S4 for tin concentration 2 mM, and S5 for tin concentration 2.4 mM.

All the spray deposited thin films were exhibited low-temperature annealing at 270°C for 40 min, followed by high-temperature annealing at 550°C for 40 min. Annealing was carried in an N_2 environment without any sulfur or tin powder.

Characterization techniques

The structural as well as phase identification measurements were carried out by an X-ray Diffractometer (GBC-XRD, EMMA) with a step size of 0.02 deg. Using a $\text{Cu}_K\alpha_1$ ($\lambda = 1.54062 \text{ \AA}$) radiation source operated at 35.5 kV and 28 mA. Elemental analysis of the CZTS thin films was done by a Scanning Electron Microscope (SEM) with dispersive electron X-ray (EDX) (Carl Zeiss, EVO 18). The optical transmittance measurements were made using a UV-VIS-NIR (Hitachi, UH4150) spectrophotometer coupled with an integrating sphere. Using a Stylus Profilometer (Bruker, DektakXT-A) thickness of the thin films was measured. Electrical properties were measured using a Hall Effect Measurement System (Ecopia, HMS-3300 with AHT55T3).

Results and discussion

The X-ray diffraction patterns of CZTS films synthesized with various tin concentrations are shown in Fig. 1. As can be seen, peaks are assigned to (112), (204), and (312) planes of the CZTS kesterite phase (according to the card JCPDS 26-0575), with (112) plane as preferential orientation in all diffraction patterns (Kumar *et al.*, 2009; Daranfedi *et al.*, 2012). Peak intensities in an XRD spectrum are the result of

total reflection from each crystal plane. Hence, it can be summarized from Fig. 1, initially the crystallinity of the thin films increases (from S1 to S3) with a tin concentration in the precursor solution and then again decreases for S4 and S5. Sample S3 has the highest intensity of kesterite phase with (112) plane as a preferential orientation.

In a quaternary compound, such as CZTS, it is hard to avoid secondary phases formation regardless of the deposition method. From Fig. 1, it can be easily observed that S1 and S5 films have lower intensity of kesterite phases compared to other secondary phases. Along with the CZTS kesterite phase, S1 film with 0.5 mM tin concentration contains Cu_3SnS_4 (JCPDS card no. 36-0218) and Cu_xS (JCPDS Card no. 36-0380) phases. Whereas, in the case of S5 with tin concentration 2.4 mM, ZnS (JCPDS card no. 10-0434) is the dominant secondary phase. It reveals that Sn concentration has to be optimized to improve the crystallinity of CZTS thin film and reduce the presence of impurity phases.

The crystallite size, D , for the fabricated CZTS thin films are calculated by using Scherrer's formula (Bashar *et al.*, 2019):

$$D = 0.9\lambda / \beta \cos\theta \quad (1)$$

where, λ ($= 1.54062 \text{ \AA}$) is the wavelength of the X-ray beam, θ is diffraction angle and β is the full width at half maximum (FWHM) of the diffraction peak.

To estimate the number of defects in the sample, the dislocation density (δ) is calculated for the samples by using the relation (Bashar *et al.*, 2019):

$$\delta = n / D^2 \quad (2)$$

where D is the crystallite size, n is a factor, which is considered almost equal to unity for minimum dislocation density. To determine the crystal imperfection and distortion induced in the samples lattice strain (ε), which is caused by the variable displacement of the atoms with respect to their reference-lattice positions, is also calculated using the Williamson-Hall formula (Bashar *et al.*, 2019):

$$\varepsilon = - \frac{\beta_{\text{int}}}{4 \tan \theta} \quad (3)$$

where θ and β have their usual significances. All these structural parameters are listed in Table I. This reveals the apparent variation in crystallite size, dislocation density, and strain value of the CZTS thin films with Sn concentration in

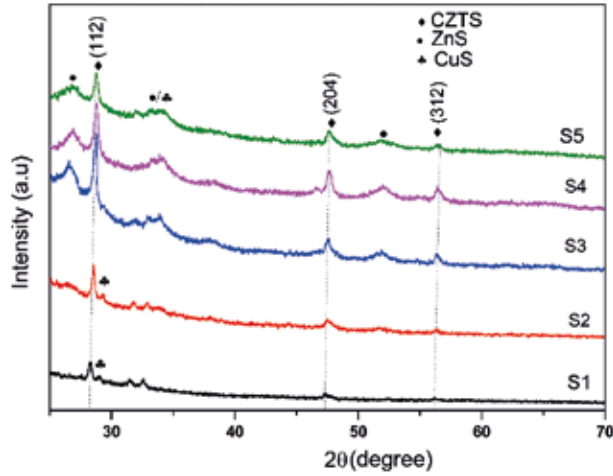


Fig. 1. XRD patterns of CZTS thin films deposited with different tin concentration

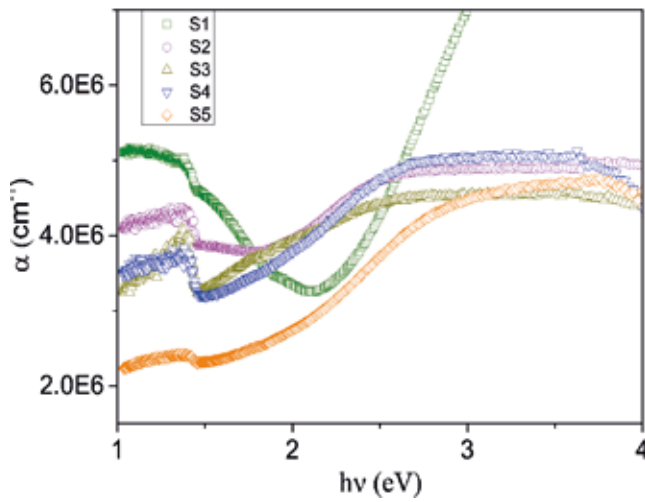


Fig. 2. Absorption coefficient as a function of photon energy for films with different tin concentration

the spray solution. Sample S3 has the largest crystallite size. Within a single crystallite, all the crystal planes are oriented in the same direction. Thus, larger crystallite size may have facilitated more significant peak intensity in the XRD spectra (Fig. 1). When the Sn concentration is more than 1.8 mM, the crystallite size of the CZTS thin film decreases. The dislocation density and strain are minima for sample S3.

The optical absorption coefficient (α) was determined from the transmittance spectra of CZTS thin films with different tin concentrations. Variation in absorption coefficient with

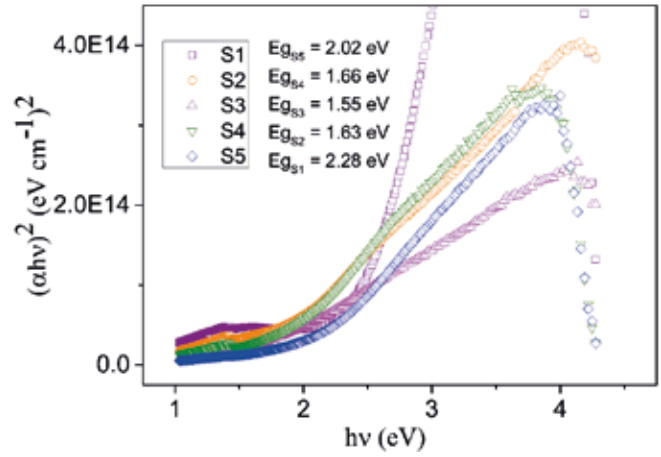


Fig. 3. $(\alpha hv)^2$ as a function of photon energy for films with different tin concentration

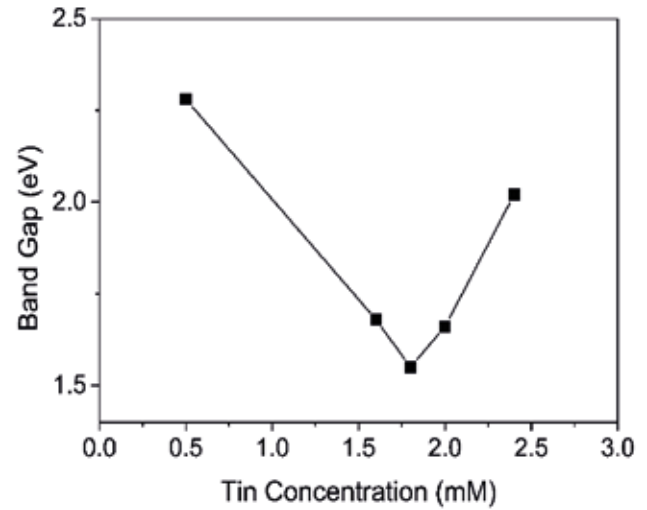


Fig. 4. Variation of band gap as a function of tin concentration in precursor solution

photon energy for different tin concentrations is presented in Fig. 2. Optical band gap values of the thin films are estimated, as shown in Fig. 3 from the plot of $(\alpha hv)^2$ as a function of photon energy hv , according to the Tauc formula for direct bandgap semiconductor (Bashar *et al.*, 2020).

$$(\alpha hv)^2 = B (hv - E_g) \quad (4)$$

Where α is the absorption coefficient, B is a constant, E_g is

Table I. Structural parameters of CZTS thin films

Sample Name	Sn Conc. (mM)	FWHM β ($^{\circ}$)	D (\AA)	δ (10^{-5}nm^{-2})	ε
S1	0.5	0.276	296.868	1.135	0.0189
S2	1.6	0.292	280.602	1.270	0.0200
S3	1.8	0.263	311.542	1.030	0.0181
S4	2.0	0.378	216.761	2.128	0.0259
S5	2.4	0.392	209.020	2.289	0.0292

Table II. Stoichiometric ratio of the spray deposited CZTS thin films

Sample name	Tin conc. (mM)	Composition of elements in atomic %				Atomic ratio Cu:Zn:Sn:S
		Cu/Zn	Cu/Sn	Zn/Sn	Cu/(Zn+Sn)	
S1	0.5	0.855	26.701	31.236	0.83	26.8:31.3:1:19.9
S2	1.6	1.824	1.298	0.711	0.76	1.9 : 1 : 1.5 : 9.8
S3	1.8	1.703	1.290	0.757	0.73	1.8 : 1 : 1.4 : 2.9
S4	2.0	0.941	0.469	0.499	0.31	1 : 1.1 : 2.2 : 2.3
S5	2.4	0.904	0.308	0.341	0.23	1 : 1.2 : 3.3 : 2

Table III. Electrical properties of the spray deposited CZTS thin films

Sample	Sn Conc.	ρ (Ωcm) $\times 10^{-3}$	μ (cm^2/Vs)	Carrier density (cm^{-3}) $\times 10^{20}$
S1	0.5	2.299	1.186	22.89
S2	1.6	5.428	4.257	2.70
S3	1.8	6.746	2.197	4.21
S4	2.0	2.193	0.492	57.89
S5	2.4	93.51	1.605	0.42

the optical gap energy, ν is incident photon energy, and h is the Plank's constant.

The variation of the deduced optical band gaps with tin concentration is reported in Fig. 4. S2, S3, and S4 have band gaps within a range of 1.5-1.6 eV, which is in good agreement with CZTS band gap values reported by other authors (Daranfed *et al.*, 2012; Diwate *et al.*, 2017). S3 has the lowest band gap 1.55 eV, which is close to the

stoichiometric value of CZTS. XRD patterns also show that S3 has a higher intensity of kesterite phases and lower intensity of other secondary phases. In comparison, S1 and S5 have wider band gaps. The presence of secondary phases in S1 and S5 was demonstrated from XRD patterns, which may cause the enlargement of the optical band gap. Also, the large optical band gap of the thin films may be a result of their composition.

The EDX results are presented in Table II. Regarding the stoichiometric ratio of CZTS thin films, sample S3 provides the best EDX result. This EDX result is also in good agreement with XRD patterns and optical data analysis. Table II reveals the presence of a lower concentration of Cu and Zn in the CZTS thin films. Hence, optimization of Cu and Zn concentration may give single-phase CZTS.

To study the electrical properties of the CZTS thin films, we carried out a Hall measurement of the samples at room temperature. Table III summarizes the electrical resistivity, mobility, and carrier concentration values for five CZTS thin film samples. It can be observed from Table III, and all the films have high carrier concentration compared to the CZTS thin films reported in (Vigil-galán *et al.*, 2013; Diwateet *et al.*, 2017).

Conclusion

In summary, CZTS absorption layers were fabricated by the spray pyrolysis method. Shallow and high concentrations of Sn content lead to the formation of secondary phases. It has been found that the spray pyrolysis solution with Sn concentration 1.8 mM (S3) has the highest structural quality of the CZTS film due to a minimum content of secondary phases. The band gap of the CZTS thin film is 1.55 eV. The elemental analysis also reveals that the sample has an atomic ration of 1.8:1:1.4:2.9, which shows minimum deviation from the standard stoichiometric ratio (2:1:1:4 for Cu, Zn, Sn and S) compared to other samples. Whereas CZTS films with low and high Sn content have secondary phases related to copper, and Zn compounds give a higher optical bandgap. The main result presented in this work concerning the evolution of secondary phases in the CZTS with the variation of Sn content in the spray solution. All the CZTS thin films have good electrical properties. The elemental analysis also shows that the CZTS thin films are Cu poor. Future work will also study the optimization of Cu and Zn content for single-phase CZTS thin film.

References

- Green MA, Yoshita M, Dunlop ED, Levi DH and Baillie AWYH (2019), Solar cell efficiency tables (version 54), *Prog. Photovolt.: Res. Appl.* **27**: 565–575, DOI: <https://onlinelibrary.wiley.com/doi/10.1002/pip.3171>.
- Mitzi DB, Gunawan O, Todorov TK, Wang K and Guha S (2011), The path towards a high-performance solution-processed kesterite solar cell, *Sol. Energy Mater. Sol. Cells*, **95**: 1421–1436, DOI: <https://doi.org/10.1016/j.solmat.2010.11.028>.
- Tanaka K, Kato M and Uchiki H (2014), Effects of chlorine and carbon on $\text{Cu}_2\text{ZnSnS}_4$ thin film solar cells prepared by spray pyrolysis deposition, *J. Alloys Compd.*, **616**: 492–497, DOI: <https://doi.org/10.1016/j.jallcom.2014.07.101>.
- Vigil-galán O, Espindola-rodríguez M, Courel M, Fontané X, Sylla D, Izquierdo-Roca V, Fairbrother A, Saucedo E and Pérez-Rodríguez A (2013), Secondary phases dependence on composition ratio in sprayed $\text{Cu}_2\text{ZnSnS}_4$ thin films and its impact on the high power conversion efficiency, *Sol. Energy Mater. Sol. Cells*, **117**: 246–250, DOI: <https://doi.org/10.1016/j.solmat.2013.06.008>.
- Vigil-galán O, Courel M, Espindola-rodriguez M, Jiménez-olarte D, Aguilar-Frutos M. and Saucedo E. (2015), Electrical properties of sprayed $\text{Cu}_2\text{ZnSnS}_4$ thin films and its relation with secondary phase formation and solar cell performance, *Sol. Energy Mater. Sol. Cells*, **132**: 557–562, DOI: <https://doi.org/10.1016/j.solmat.2014.10.009>.
- Babichuk IS, Golovynskyi S, Brus VV, Babichuk IV, Datsenko O, Li J, Xu G, Golovynska I, Hreshchuk OM, Orletsky IG, Qu J, Yukhymchuk VO, Maryanchuk PD, Secondary phases in $\text{Cu}_2\text{ZnSnS}_4$ films obtained by spray pyrolysis at different substrate temperatures and Cu contents, *Mater. Lett.*, **216**: 173–175, DOI: <https://doi.org/10.1016/j.matlet.2018.01.010>.
- Bhosale SM, Suryawanshi MP, Gaikwad MA, Bhosale PN, Kim JH and Moholkar AV (2014), Influence of growth temperatures on the properties of photoactive CZTS thin films using spray pyrolysis technique, *Mater. Lett.*, **129**: 153–155, DOI: <https://doi.org/10.1016/j.matlet.2014.04.131>.
- Mahjoubi S, Bitri N, Bouzouita H, Abaaband M and Ly I (2017), Effect of the annealing and the spraying time on the properties of CZTS thin films prepared by the "Spray sandwich" technique, *Appl. Phys. A*, **123**: 452, DOI: <https://doi.org/10.1007/s00339-017-1020-4>.
- Bashar MS, Matin R, Sultana M, Siddika A, Rahaman M, Gafur MA and Ahmed F (2020), Effect of rapid thermal annealing on structural and optical properties of ZnS

thin films fabricated by RF magnetron sputtering technique, *J. Theor. Appl. Phys.*, **14**: 53-63, DOI: <https://doi.org/10.1007/s40094-019-00361-5>.

Daranfed W, Aida MS, Attaf N, Bougdira J and Rinnert H (2012), "Cu₂ZnSnS₄ thin films deposition by ultrasonic spray pyrolysis", *J. Alloy Compd.*, **542**: 22-27, DOI: <http://dx.doi.org/10.1016%2Fj.jallcom.2012.07.063>.

Bashar MS, Yulisa Y, Abdullah SF, Rahaman M, Chelvanathan P, Gafur A, Ahmed F, Akhtaruzzaman M and Amin N (2020), "An investigation on structural and optical properties of Zn_{1-x}Mg_xS thin films deposited by

RF magnetron co-sputtering technique", *Coatings*, 10: 766, DOI: <https://doi.org/10.3390/coatings10080766>.

Diwate K, Mohite K, Shinde M, Rondiya S, Pawbake A, Date A, Pathan H and Jadkar S (2017), Synthesis and characterization of chemical spray pyrolysed CZTS thin films for solar cell applications, *Energy Procedia* **110**: 180-187, DOI: <https://doi.org/10.1016/j.egypro.2017.03.125>.